# FITTING THE SPECTRA OF PIONS, KAONS, PROTONS, AND ANTIPROTONS IN RELATIVISTIC CU + CU COLLISIONS

**[1]M. M. Sultanov, [2]A. N. Jumanov[*], [3]A. A. Usarov, [4]Q. Kh. Yakhshiboyev**
Jizzakh Politechnical Institute, Uzbekistan[1], Samarkand State Medical Institute, Uzbekistan[2], Academic Lyceum under Samarkand State Architectural and Building Institute[3]
amattou@rambler.ru

---

## ABSTRACT

By the BRAHMS collaboration investigated the spectra of Pions, Kaons, protons, and antiprotons in relativistic Cu + Cu at an energy of $\sqrt{S_{MN}}$ =200 GeV/s at the rapidity values y=0 and y=3. It was found that with an increase in the centrality of collisions, the collective radial flux of particles increases and the freeze-out temperature decreases.

1. 5 GeV / c <$p_t$ <2. 5 GeV / c, the yield of Pions and Kaons is suppressed than in p + p collisions at the same energy. In this work, the experimentally obtained particle spectra are fitted by the Levy function and the exponential function of the Boltzmann type. It is shown that the fitted spectra of Pions by the Levy function and the spectra of Kaons and protons with an exponential function describe the experimental data well.

***Keywords: Pion, Kaon, proton, antiproton, quark, gluon, plasma, tranversal, momentum, temperature, exponential, centrality.***

## INTRODUCTION

There are two main problems in quantum chromodynamics (QCD) related to the vacuum structure that can only be solved by relativistic nuclear physics. These problems are: color charge configuration and spontaneous disruption of chiral symmetry. The confinement means that there are no colored objects in the observed spectrum of hadron states. From the point of view of quarks-gluons' assumptions about the structure of hadrons, the confinement means that quarks and gluons cannot propagate at distances greater than 1fm (hadron size) [1]. However, this assertion is valid only at normal nuclear densities. The high-density nuclear material formed in the collisions of relativistic nuclei occurs in the deconfusion phase, that is, the generalization of quarks and gluons belonging to a single nucleon. can be spread over distances up to the size. Spontaneous disruption of chiral symmetry means the following. At the limit of the mass of the quarks close to zero, in the QCD this limit is fully valid for the quarks u and d. Because mu, d << mp << mN, the right and left components of their QCD lagrangian are different from each other, and the vector gluons do not mix with each other. The QCD vacuum is chiral asymmetric due to the presence of a π-meson with almost no mass relative to other hadrons and a negative internal pair. Thus, at zero temperature and normal core densities, the QCD vacuum is configurable and is in a state of disturbed chiral symmetry.

## A brief description of the experimental device and the results obtained

Today, the most pressing problems of microcosm physics are being solved in giant colliders with energies of accelerating nuclei up to a few TeV. Depending on their structure, colliders come in a variety of design solutions. Colliders are giant blocking complexes in which particles or ionized heavy nuclei (e.g., Au, Pb, U) reach speeds of up to several tens of kilometers in length. Typically, colliders consist of two synchrotrons with a single ring, in which the same charged ions are accelerated in opposite directions, and the meeting points of these bundles in orbit are formed in the area where the experimental devices - detectors are installed. A nuclear reaction occurs as a result of the collision of heavy ions forming opposite bundles. One such collider is the RHIC (Relativistic Heavy Ion Collider) at the Brookhaven National Laboratory in the United States, which

accelerates the Cu, Au, and Pb nuclei. The RHIC orbit is 3834 m long and has a one-way acceleration energy of 100 GeV / nucleon, launched in 2000.

In RHIC, nuclei such as gold (Au) and uranium (U) collide with 200 GeV energy per nucleon. [2]. Such collisions result in an opaque environment composed of partons, strongly bonded, elongated, and reflecting a hydrodynamic flow. This medium is called strongly bound quark-gluon plasma (QGP).

Matter formed by the collision of heavy ions has a very short lifespan. After the collision, it expands and then cools with the conversion of all the particles into hadrons (adronization), and some of them can be recorded experimentally by wires through detectors as wires or leading hadrons (e.g., high-energy π-mesons). The QGP matter can be studied by comparing the spectra of sample particles formed in the collision of heavy ions with the spectra of particles formed in the p + p collisions of the same energy. In the measurement of narrow and leading hadrons, it is assumed that the sample formed in the initial state of the particle-dense medium. The observer's task is to provide information about the initial state of the low-energy hadron system and its evolution. Conducting such observations systematically as a function of the Hadrons involved in the collision ($N_{part}$) is very important in understanding the properties and state of matter formed in the collision Au + Au with energy $\sqrt{S_{NN}}$=200 GeV. However, in Au + Au peripheral collisions with $N_{part}$ <60, the error in detecting $N_{part}$ is around 20% [3,4]. In this case, the particles leave the collision field in different scenarios, depending on their origin.

## Particle spectra and their fit

The elongation of the size of relatively small systems such as Cu + Cu, where physically observed d + Au and p + p, $A_{Cu}$ = 63, is separated by the amount of particles involved in well-shielded peripheral Au + Au collisions. The uncertainty in the Cu + Cu collision sections is rarely compared to the Au + Au collisions in the same number of participants. Assuming that the mass distribution is isotropic, the area of the shield will be spherical at Cu + Cu central collisions. The shape of the system in the Au + Au collision, in which a similar participant exists, is in the form of an alloy (cocoon), which allows to study the geometric effects in experimental observations.

E-ISSN NO:2349-0721

Most of the data on the recorded hadrons are based on average speeds. BRAHMS data offer a great way to increase our knowledge of matter formation and various chemical conditions by studying the hadrons formed at both average velocities and anterior velocities, comparing their properties. $\sqrt{S_{NN}}$=200 GeV The transverse pulse pt spectra of charged hadrons ($\pi^{\pm}$, $K^{\pm}$, p, ṕ ) in collisions with energy $\sqrt{S_{NN}}$=200 GeV Cu + Cu were measured as a function of the collision center at velocity y = 0 and y = 3. The results were compared with those obtained at p + p and Au + Au collisions with the same energy, velocity, and centrality (number of participating particles).

In the case of elementary p + p and p + ṕ collisions, the spectra of hadrons are expressed by the peturbatic QCD for $p_t$ ~ 2 GeV [5-7]. The data on Cu + Cu collisions in this paper cover the lower physics field as well as the high pt-transition phenomenon. In this study, we study the origin of such a transition, first by studying the global hydrodynamic properties of the system using blast wave fits, secondly by generating a complete output for each particle type and $<p_t>$ average transverse impulse, and thirdly by different is expressed by showing the particle ratio as a function of $p_t$ and, finally, by summing the nuclear variability (RAA) factor as a function of $p_t$ and velocity.

The process of determining the collision center in the Cu + Cu system is described in detail in the study of Au + Au collisions using the amount of particle $<N_{part}>$ and sequential colliding nucleons $<N_{coll}>$ [8]. The values obtained during the process are given in Table 1. For this analysis, events were divided into 4 central areas: 0-10%, 10-30%, 30-50%, and 50-70%. Events within ± 25 cm of the nominal collision point were selected.

Table 1. Values of $<N_{part}>$ and $<_{Ncoll}>$ quantities for Cu + Cu collision centrality area

| centrality | $<N_{part}>$ | $<N_{coll}>$ |
|---|---|---|
| 0-10% | 97±0,8 | 166±2 |
| 10-30% | 61±02,6 | 85±5 |
| 30-50% | 29±4,3 | 30±6 |
| 50-70% | 12±3,2 | 9. 6±3,2 |

Measuring the transverse momentum $p_t$ spectrum of secondary particles formed by the collision of heavy ions is the first and most important step in the study of a number of quantities that reflect the properties of the particle medium.

Table 2. Results of fitting $\pi^+$-meson with Levi function. The fitting area is 0.35 GeV / c < $p_t$ < 2.0 GeV / c at y = 0 and 0.45 GeV / c <$p_t$ <2.0 GeV / c at y = 3.

| | centrality | dN/dy | $(dN/dy)_m$ | $N_m/N$ | $<p_t>$, MeV | $\chi^2$/EDS | $n_0$ | *T*, MeV |
|---|---|---|---|---|---|---|---|---|
| y=0 | 0-10% | 81,1±3,1±5,9 | 42,1 | 0. 52 | 454±2±21 | 0,2/9 | 12,8 | 172 |
| | 10-30% | 48,0±2,1±3,5 | 24,3 | 0,51 | 445±4±21 | 0,9/9 | 11,6 | 164 |
| | 30-50% | 21,8±0,5±1,6 | 10,8 | 0,50 | 438±2±21 | 0,2/9 | 11,2 | 159 |
| | 50-70% | 8,5±0,40±0,62 | 4,0 | 0,47 | 418±5±20 | 2,4/9 | 10,2 | 147 |
| y=3 | 0-10% | 33,7±3,5±3,0 | 11,2 | 0,33 | 401±8±26 | 12,2/9 | 17,0 | 159 |
| | 10-30% | 18,3±1,9±1,6 | 6,6 | 0,36 | 424±9±28 | 16,2/9 | 19,3 | 173 |
| | 30-50% | 9,3±0,88±0,83 | 3,1 | 0,33 | 403±7±26 | 7,3/9 | 16,1 | 158 |
| | 50-70% | 3,3±,0,70±0,29 | 1,2 | 0,35 | 418±14±27 | 23,0/9 | 17,9 | 168 |

E-ISSN NO:2349-0721

Table 3. Results of fitting $\pi^-$-mesons with Levi function. The fitting area is 0.35 GeV / c < $p_t$ < 2.0 GeV / c at y = 0 and 0.45 GeV / c <$p_t$ <2.0 GeV / c at y = 3

| | centrality | dN/dy | $(dN/dy)_m$ | $N_m/N$ | $<p_t>$,MeV | $\chi^2$/EDS | $n_0$ | *T*, MeV |
|---|---|---|---|---|---|---|---|---|
| y=0 | 0-10% | 78,0±3,3±4,9 | 41,1 | 0,53 | 460±4±22 | 0,9/9 | 13,3 | 176 |
| | 10-30% | 44,7±1,9±2,8 | 23,2 | 0,52 | 455±5±21 | 2,1/9 | 12,3 | 170 |
| | 30-50% | 20,5±0,9±1,3 | 10,2 | 0,50 | 441±3±21 | 0,5/9 | 10,6 | 158 |
| | 50-70% | 8,0±0,36±0,51 | 3,8 | 0,47 | 421±4±20 | 0,7/9 | 10,2 | 148 |
| y=3 | 0-10% | 32,4±3,1±2,9 | 11,2 | 0,35 | 411±8±27 | 14,5/9 | 17,5 | 164 |
| | 10-30% | 20,8±1,8±1,8 | 7,4 | 0,36 | 419±8±27 | 13,9/9 | 21,0 | 173 |
| | 30-50% | 11,1±1,4±1,0 | 3,5 | 0,32 | 392±9±25 | 16,8/9 | 15,5 | 152 |
| | 50-70% | 3,6±0,40±0,32 | 1,3 | 0,36 | 424±8±28 | 5,2/9 | 20,5 | 174 |

Systematic study of spectra requires fitting them with various functions. Fitting the spectrum of Pions with the Levi function of the form $A\cdot(1+\frac{m_T-m_0}{n_0T})^{-n_0}$ gives good results [9-11]. The fitting results are given in Tables 2 and 3.

For Kaons and protons, it was found expedient to fit the spectra with the Boltzmann exponential function in the form $A\cdot m_T e^{-\frac{m_T}{T}}$. For the Boltsman function, the T fitting parameter can be taken as the effective

temperature of the system. The fact that the transverse pulse area of pt obtained for fitting with the Levi function is much wider than the area of fitting with $p_t$ using the Boltzmann function allows for better detection of pon output and $<p_t>$.

During the fitting process, the weights were obtained as the sum of the squares of statistical errors and the systematic errors at the points. The fit area (spacing) fit parameters, number of degrees of freedom (EDS) and $\chi^2$/ EDS values are given in Tables 4, 5, 6 for Pions, Kaons and protons. The total value of the output dN / dy and the average value of the transverse pulse <pt> were obtained by extrapolation outside the measurement range of the fit function. The total value of the output dN / dy and the average value of the transverse pulse $<p_t>$ were obtained by extrapolation outside the measurement range of the fit function. The dominant uncertainties in the results of the magnitudes dN / dy and $<p_t>$ arise from extrapolating the spectrum to $p_t = 0$. They are evaluated by the different form of the function in the fit and by the area of the $p_t$. For Peons and Kaons, extrapolation to $p_t = 0$ is more pronounced at y = 3 than at y = 0. Because the lower limit of the $p_t$ field is much higher than in the case of y = 3. This effect increases systematic uncertainties in the anterior spectra. Some of the emitted particles are recorded in BRAHMS by the spectrometer and around 30-75% depending on the type of particles.

For average velocity and pre-velocity data, the spectra of pion, kaon, proton, and antiproton were simultaneously fitted with three parameters: $T_{kin}$, $\beta_s$, and α. The normalization parameter was obtained by fitting the data set. Particles formed from resonances and with an impulse below 0.4 GeV / c were not taken into account, as the effects caused by them are almost imperceptible. The fit area is $p_t$ <1.8 GeV / c for Peons, $p_t$ <2.0 GeV / c for Kaons,

$p_t$ <3.0 GeV / c for protons.

Table 4. Results of fitting $K^+$-mesons with $m_T$-dependent exponential function. The fitting area is 0.45 GeV / c < $p_t$ <2.0 GeV / c at y = 0 and 0.75 GeV / c < $p_t$ <2.5 GeV / c at y = 3.

| | centrality | dN/dy | $(dN/dy)_m$ | $N_m/N$ | $<p_t>$, MeV | $\chi^2$/EDS | *T*, MeV |
|---|---|---|---|---|---|---|---|
| y=0 | 0-10% | 12,3±0,32±0,89 | 7,6 | 0,62 | 674±10±22 | 1,6/7 | 277 |
| | 10-30% | 6,9±0,01±0,50 | 4,2 | 0,61 | 663±7±21 | 0,9/7 | 271 |
| | 30-50% | 2,8±0,02, ±0,20 | 1,7 | 0,62 | 663±7±21 | 3,9/7 | 273 |
| | 50-70% | 1,0±0,05±,0,12 | 0,6 | 0,59 | 625±14±20 | 3,4/7 | 251 |
| y=3 | 0-10% | 4,6±0,29±0,36 | 1,3 | 0,27 | 611±14±20 | 4,1/4 | 244 |
| | 10-30% | 3,0±0,20±0,23 | 0,78 | 0,26 | 594±19±19 | 5,8/4 | 235 |
| | 30-50% | 1,4±0,11±0,11 | 0,34 | 0,25 | 577±20±18 | 5,7/4 | 226 |
| | 50-70% | 0,39±0,05±0,03 | 0,10 | 0,26 | 600±27±19 | 5,4/4 | 238 |

Table 5. Results of fitting $K^+$-mesons with $m_T$-dependent exponential function. The fitting area is 0.45 GeV / c < $p_t$ <2.0 GeV / c at y = 0 and 0.75 GeV / c < $p_t$ <2.5 GeV / c at y = 3.

| | centrality | dN/dy | $(dN/dy)_m$ | $N_m/N$ | $<p_t>$,MeV | $\chi^2$/EDS | *T*, MeV |
|---|---|---|---|---|---|---|---|
| y=0 | 0-10% | 11,2±0,23±0,71 | 7,2 | 0,64 | 6829±22 | 2,0/8 | 282 |
| | 10-30% | 6,1±0,15±0,38 | 3,9 | 0,64 | 683±12±22 | 4,3/8 | 282 |
| | 30-50% | 2,5±0,08±0,16 | 1,6 | 0,63 | 677±26±22 | 11,4/8 | 279 |
| | 50-70% | 0,7±0,02±0,10 | 0,5 | 0,64 | 685±28±22 | 10,8/8 | 283 |
| y=3 | 0-10% | 3,9±0,02±0,30 | 0,96 | 0,25 | 569±12±18 | 5,5/5 | 222 |
| | 10-30% | 2,2±0,12±0,17 | 0,57 | 0,26 | 580±10±19 | 4,4/5 | 227 |
| | 30-50% | 1,0±0,05±0,08 | 0,24 | 0,23 | 551±12±18 | 4,8/5 | 213 |
| | 50-70% | 0,34±0,02±0,03 | 0,08 | 0,25 | 572±12±18 | 1,5/5 | 223 |

Table 6. Results of fitting protons with $m_T$-dependent exponential function. The fitting area is 0.55 GeV / c < $p_t$ <2.0 GeV / c at y = 0 and 0.75 GeV / c < $p_t$ <2.5 GeV / c at y = 3.

| | centrality | dN/dy | $(dN/dy)_m$ | $N_m/N$ | $<p_t>$,MeV | $\chi^2$/EDS | *T*, MeV |
|---|---|---|---|---|---|---|---|
| y=0 | 0-10% | 8,1±0,03±0,51 | 5,7 | 0,70 | 896±18±29 | 9,1/9 | 332 |
| | 10-30% | 4,7±0,10±0,29 | 3,2 | 0,69 | 874±9±28 | 1,9/9 | 320 |
| | 30-50% | 2,1±0,05±0,13 | 1,4 | 0,67 | 831±14±27 | 6,4/9 | 296 |
| | 50-70% | 0,7±0,03±0,05 | 0,46 | 0,64 | 784±25±25 | 12,3/9 | 271 |
| y=3 | 0-10% | 7,0±0,03±0,44 | 5,1 | 0,74 | 775±13±25 | 10,3/10 | 266 |
| | 10-30% | 4,3±0,11±0,27 | 3,2 | 0,73 | 761±16±24 | 12,4/10 | 259 |
| | 30-50% | 2,0±0,07±0,12 | 1,4 | 0,71 | 737±38±24 | 23,2/10 | 247 |
| | 50-70% | 0,76±0,04±0,05 | 0,54 | 0,70 | 712±57±23 | 30,7/10 | 234 |

Table 7. Results of fitting antiprotons with $m_T$-dependent exponential function. The fitting area is 0.55 GeV / c < $p_t$ <2.0 GeV / c at y = 0 and 0.75 GeV / c < $p_t$ <2.5 GeV / c at y = 3.

| | centrality | dN/dy | $(dN/dy)_m$ | $N_m/N$ | $<p_t>$,MeV | $\chi^2$/EDS | *T*, MeV |
|---|---|---|---|---|---|---|---|
| y=0 | 0-10% | 6,0±0,17±0,38 | 4,3 | 0,70 | 906±38±29 | 15,9/9 | 338 |
| | 10-30% | 3,5±0,11±0,22 | 2,4 | 0,69 | 880±12±28 | 3,9/9 | 323 |
| | 30-50% | 1,5±0,04±0,10 | 1,0 | 0,68 | 839±16±27 | 7,7/9 | 300 |
| | 50-70% | 0,6±0,02±0,04 | 0,38 | 0,64 | 781±22±25 | 10,9/9 | 269 |
| y=3 | 0-10% | 1,2±0,04±0,07 | 0,73 | 0,62 | 750±20±24 | 11,7/9 | 254 |
| | 10-30% | 0,86±0,04±0,05 | 0,53 | 0,61 | 731±31±23 | 17,1/9 | 244 |
| | 30-50% | 0,37±0,01±0,02 | 0,22 | 0,60 | 719±27±23 | 14,2/9 | 238 |
| | 50-70% | 0,15±0,01±0,01 | 0,09 | 0,57 | 685±42±22 | 18,2/9 | 221 |

The lines in Figure 2 are the result of fitting. Continuous lines indicate the cross-sectional area for fitting, and dashed lines represent the results of extrapolation of functions in the fitting area.

Figure 1 shows the correlation between the kinetic temperature $T_{kin}$ and the average transverse velocity $<\beta> = \frac{2}{\alpha+2} \cdot \beta_s$ for central collisions at both velocity values (y = 0 and y = 3). An increase in centrality of collision is observed a decrease $T_{kin}$ with the increases <b>. This means that the extended system will last longer. As the system cools due to the random thermal action of the partons, they move to a volumetric radial flow with a loss of temperature and increase the average velocity.

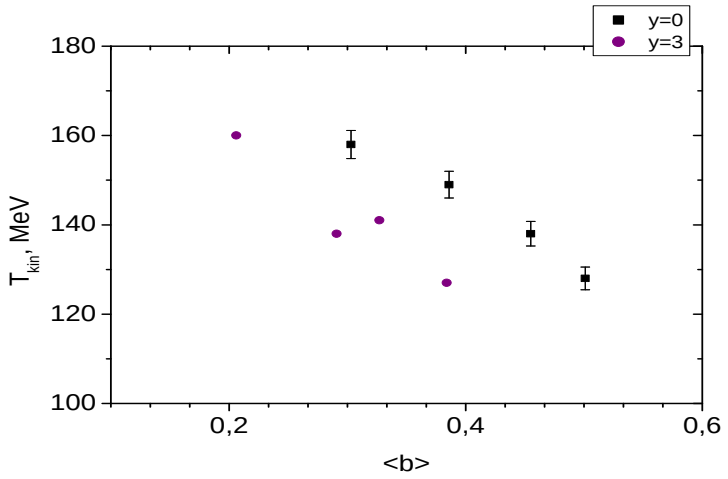


Fig.1. The relationship between the kinetic energy $T_{kin}$ and the average transverse velocity <b> of the blast wave fit parameters in a Cu + Cu collision with energy $\sqrt{S_{NN}}$ = 200 Gev/c

.

Although the $T_{kin}$ lines are similar in the case of y = 0 and y = 3, a slight reversal occurs at <β>~0.3 (y = 3), indicating that the temperature is as low as about 20 MeV and that y = 3 indicates that the particle density is likely to be low. For a given dN / dy, the magnitudes $T_{kin}$ and <β> are small when y = 3 (a small energy is recorded) and represent matter at an anterior velocity. In the Cu + Cu and Au + Au reactions, the dependence of the dN / dy variable on the $T_{kin}$ and <β> magnitudes is very similar, with the kinetic energy slightly higher and the mean velocity slightly lower.

## CONCLUSION

The transverse pulse pt spectra of charged hadrons ($\pi^{\pm}$, $K^{\pm}$, p, $\acute{p}$ ) in $\sqrt{S_{NN}}$=200 GeV energy Cu + Cu collisions are of the form $A\cdot(1+\frac{m_T-m_0}{n_0T})^{-n_0}$ very well fit with the Levi function and the Boltzmann exponential function in the form $A\cdot m_T e^{-\frac{m_T}{T}}$.

As the number of particles $N_{part}$ increases, the $T_{kin}$ temperature decreases and the velocity increases. For a given <β>, the kinetic energy of $T_{kin}$ is 15-20 MeV lower than in the case of
y = 0 at y = 3. The dN / dy value of Kaons for $N_{part}$ is slightly smaller than that of Au + Au in
Cu + Cu collisions.

In Cu + Cu collisions, the release of Pions and Kaons is much more complicated than in p + p collisions. This complexity also intensifies with increasing centrality of collisions. This phenomenon is especially noticeable at the front speed.

## REFERENCES

1. Emelyanov V. M. , Timoshenko S. L. , Strixanov M. N. Introduction to relativistic nuclear physics. M. , Fizmatlit-2004
2. Kh. Olimov et al. Average transverse expansion velocities and global freeze-out temperatures in central Cu + Cu, Au + Au, and Pb + Pb collisions at high energies at RHIC and LHC. Modern Physics Letters A. Vol. 35, No. 14 (2020) 2050115 (25 pages).
3. S. Adler et al. (PHENIX), Phys. Rev. C69,034909 (2004). Adareetal. (PHENIX), Phys. ReV. C88, 024906 (2013).
4. F. Abe et al. (CDF), Phys. Rev. Lett. 61, 1819 (Oct. 1988).
5. S. Adler et al. (PHENIX Collaboration), Phys. Rev. C69, 0344910 (Mar. 2004).
6. A.Adare et al. (PHENIX Collaboration), Phys. Rev. D 76, 051106 (Sep. 2007).
7. Bearden et al. (BRAHMS), Phys. Rev. Lett. 88, 202301 (2002).
8. G. Wilk and Z. Wlodarczyk, Phys. Rev. Lett. 84, 2770 (2000).
9. Adams et al. (STAR), Phys. Rev. C71, 064902, (2005).
10. Adare et al. (PHENIX), Phys. Rev. D83, 052004, (2011).